

DOI: 10.11931/guihaia.gxzw201803015

引文格式: 张梵, 皮秀权, 王晓娥, 等. 菰适应湿地环境的解剖和屏障结构特征研究 [J]. 广西植物, 2019, 39(5): 615–623.
ZHANG F, PI XQ, WANG XE, et al. Anatomy and apoplastic barrier histochemistry characteristics of *Zizania latifolia* adapted to wetland environment [J]. *Guihaia*, 2019, 39(5): 615–623.

菰适应湿地环境的解剖和屏障结构特征研究

张 梵^{1,3}, 皮秀权², 王晓娥^{1,3}, 杨朝东^{1,3}, 周存宇^{1,3*}

(1. 长江大学 教育部长江中游湿地农业工程研究中心, 湖北 荆州 434025; 2. 利川市农业局, 湖北 利川 445400; 3. 长江大学 植物生态与环境修复研究所, 湖北 荆州 434025)

摘 要: 菰(*Zizania latifolia*)是一种多年生挺水植物,为了探讨该植物根、茎和叶的解剖结构、组织化学及其质外体屏障的通透性生理。该文利用光学显微镜和荧光显微镜,对菰的根、茎、叶进行了解剖学和组织化学研究。结果表明:(1)菰不定根解剖结构由外而内分别为表皮、外皮层、单层细胞的厚壁机械组织层、皮层、内皮层和维管柱;茎结构由外而内分别为角质层、表皮、周缘厚壁机械组织层、皮层、具维管束的厚壁组织层和髓腔。叶鞘具有表皮和具维管束皮层,叶片具有表皮,叶肉和维管束。(2)不定根具有位于内侧的内皮层及其邻近栓质化细胞和外侧的外皮层组成的屏障结构;茎具内侧厚壁机械组织层,外侧的角质层和周缘厚壁机械组织层组成的屏障结构,屏障结构的细胞壁具凯氏带、木栓质和木质素沉积的组织化学特点,叶表面具有角质层。(3)菰通气组织包括根中通气组织,茎、叶皮层的通气组织和髓腔。(4)菰的屏障结构和解剖结构是其适应湿地环境的重要特征,但其茎周缘厚壁层和厚壁组织层较薄。由此推测,菰适应湿地环境,但在旱生环境中分布有一定的局限性。

关键词: 菰, 解剖结构, 质外体屏障结构, 组织化学, 通透性

中图分类号: Q944 文献标识码: A 文章编号: 1000-3142(2019)05-0615-09

Anatomy and apoplastic barrier histochemistry characteristics of *Zizania latifolia* adapted to wetland environment

ZHANG Fan^{1,3}, PI Xiuquan², WANG Xiao'e^{1,3}, YANG Chaodong^{1,3}, ZHOU Cunyu^{1,3*}

(1. *Engineering Research Center of Wetland Agriculture in Central Yangtze, Ministry of Education, Yangtze University, Jingzhou 434025, Hubei, China*; 2. *Lichuan Municipal Bureau of Agriculture, Lichuan 445400, Hubei, China*; 3. *Institute of Plant Ecology and Environmental Restoration, Yangtze University, Jingzhou 434025, Hubei, China*)

Abstract: Wild rice (*Zizania latifolia*) is a famous, perennial, emergent vegetable in China. The current work explores the anatomy and histochemistry of roots, stems and leaves and the permeability of apoplastic barriers of wild rice. The anatomy and histochemistry of *Z. latifolia* were studied by optical microscope and fluorescence microscope. Sections were stained with

收稿日期: 2018-05-17

基金项目: 教育部湿地生态与农业利用工程研究中心开放基金(KF201603) [Supported by Engineering Research Center of Ecology and Agriculture Use of Wetland, Ministry of Education Opening Fund(KF201603)]。

作者简介: 张梵(1994-),女,河南新乡人,硕士研究生,研究方向为植物结构与生理,(E-mail)1045420095@qq.com。

*通信作者: 周存宇,博士,硕士研究生导师,研究方向为植物生态学,(E-mail)zhoucy@yangtzeu.edu.cn。

Sudan red 7B for suberin lamellae, berberine hemisulfate-aniline blue for Casparian bands and lignified walls, and phloroglucinol-HCl (Pg) for lignin. The results were as follows: (1) The adventitious roots in wild rice suberized and lignified endodermis and adjacent, thick-walled cortical layers and suberized and lignified hypodermis, composed of a uniseriate sclerenchyma layer underlying uniseriate exodermis; The stems of wild plants included stolons, rhizomes, and culm. Rhizomes, stolons, and culms had two rings of thickened, lignified cells, the peripheral mechanical ring and the sclerenchyma ring; The latter delimits the cortex from the CC (central cylinder) and was usually associated with vascular bundles; Stems had thick epidermal cuticle, a narrow peripheral mechanical ring, cortex, sclerenchyma ring with vascular bundles and pith cavity from the outside and inside. Leaf sheaths had epidermis and cortex with vascular bundles, and leaf blades had epidermis, mesophyll and vascular bundles. (2) Apoplastic barriers were found in roots and stems. The apoplastic barriers consist of that adventitious roots had endodermis, adjacent suberized cells and exodermis; Stems have cuticle, suberized and lignified peripheral mechanical ring and sclerenchyma ring, and the cell wall of apoplastic barriers had Casparian band, lignin and suberin. Leaves had cuticles at surface. (3) The air space consist of aerenchyma in roots, and pith cavities and aerenchyma in stems and leaves. (4) The peripheral mechanical ring and sclerenchyma ring were thinner in wild rice stems that adapt to wetland environment, but limited distribution to drought environment.

Key words: *Zizania latifolia*, anatomical structure, apoplastic barriers, histochemistry, permeability

菰 (*Zizania latifolia*) 是禾本科稻亚科稻族植物之一, 与水稻 (*Oryza sativa*) 同族 (Judziewicz & Clark, 2007), 是一种重要的水生植物, 其籽粒与北美菰 (*Zizania aquatica*) 一样可作为谷物食用 (Sculthorpe, 1967)。菰具多年生根状茎、匍匐茎和地上茎, 地上茎具宽大叶片。菰沉水部分适应湿地环境的研究相对缺乏。早期曾对北美菰的根有一些研究 (Stover, 1928), 其后又有少量的关于该属植物 (包括菰和北美菰) 根和茎的解剖结构研究 (Stover, 1951; Metcalfe, 1960; Jorgenson et al., 2013; Tateoka, 1969), 而对其叶解剖的研究则较为深入 (Metcalfe, 1960)。然而, 相比其他重要草本具鳞叶的根状茎和匍匐茎植物, 稻亚科中的水稻不定根研究最多 (Tateoka, 1969; Colmer, 2003; Kawai et al., 1998; Kotula et al., 2009), 水稻茎有栓质化的内皮层 (Metcalfe, 1960)。

湿地草本植物的重要特征是具有质外体屏障, 包括根的内皮层, 外皮层和表皮 (Armstrong et al., 2006; Seago et al., 1999; Soukup et al., 2007; Armstrong et al., 2000), 以及茎叶中的厚壁机械组织层 (SCR) 和周缘厚壁机械组织层 (PMR), 如狗牙根 (*Cynodon dactylon*)、双穗雀稗 (*Paspalum distichum*) 等植物的茎具木质化和栓质化的厚壁机械组织层和周缘厚壁机械组织层及角质层, 屏障结

构是植物控制植物内部以及与环境的水、离子和氧气扩散和交换的保护组织 (杨朝东等, 2013; Enstone et al., 2002)。例如, 水稻在静止溶液培养条件下, 促进了根内、外皮层细胞壁栓质和木质素沉积的提早和增加, 更有效地阻碍离子透过 (Ranathunge et al., 2011)。这类湿地植物体内都具有发达的通气组织, 为水淹胁迫下的植物提供氧气, 包括根部通气组织 (Seago et al., 2005; Jung et al., 2008)、茎的髓腔和皮层通气组织 (Armstrong et al., 2006)。

除稻属 (*Oryza*) 外, 前人对其他稻亚科植物适应湿地环境的结构特征的研究非常有限, 菰适应而且广泛分布于湿地环境, 而不像狗牙根、双穗雀稗等也能忍耐旱生环境 (Yang et al., 2011), 菰对江汉平原农业污染环境的修复, 和对三峡库区退化湿地的恢复具有重要价值。因此, 我们对菰的根、茎和叶的解剖学和组织化学特征以及质外体屏障的通透性开展了研究, 将明确菰适应湿地环境和分布局限性的结构特征。

1 材料与方 法

于 2017 年夏季, 自湖北省江汉平原湿地采集菰的野生植株, 用自来水洗干净, 剪取不定根, 并

采用 FAA 固定(Jensen, 1962)。用新鲜的根和根状茎进行质外体渗透试验。用双面刀片在距不定根根尖 5、10、30、50、70、90 mm, 匍匐茎、根状茎和叶的幼嫩与成熟部位处分别切片。菰幼茎取自刚刚开始伸长的节间, 老茎取自于剥去叶鞘或叶片的具有髓腔的节间部位。

在解剖镜下用双面刀片对菰的根、茎、叶等样品进行徒手切片。切片染色首先用苏丹 7B (SR7B) 检验栓质化 (Brundrett et al., 1991); 然后用硫氰酸黄连素-苯胺蓝 (BAB) 检验凯氏带和木质化的细胞壁 (Seago et al., 1999; Brundrett et al., 1988), 盐酸-间苯三酚 (PG) 检验木质化 (Jensen, 1962); 最后用甲苯胺蓝 (TBO) 染色, 观察细胞结构特点。在复式光学显微镜和荧光显微镜下进行显微拍照。

不定根和根状茎的质外体通透性试验按以下步骤进行。切取 30~40 mm 长的根段, 用纸巾擦干, 用正在冷却的熔融石蜡密封其两端。根茎样品切取两端有节的节间, 两端不密封。分别取上述不定根和根状茎的切段各 5 个, 用黄连素示踪法进行质外体通透性测试。将上述切断先用 0.05% 黄连素硫酸盐滴染 1 h 后, 再用 $4.85 \times 10^3 \mu\text{g} \cdot \text{mL}^{-1}$ 硫氰酸钾溶液染色 1 h。对以上处理后的样品进行徒手切片, 置于荧光显微镜下观察 (Seago et al., 1999; Meyer et al., 2009; Meyer & Peterson, 2011)。

2 结果与分析

2.1 不定根结构和组织化学

距菰不定根根尖 5 mm 处, 其解剖结构由外而内依次为表皮、由双层细胞构成的皮下层、外层细胞环、正在发育的裂溶生性通气组织、皮层、内皮层、维管柱 (其中原生木质部和后生木质部正在分化) (图 1:A); 距根尖 10 mm 处, 在单层细胞构成的外皮层的径向壁上出现微弱的凯氏带, 由小的木质化细胞构成的皮下厚壁细胞层 (SC) 和原生木质部出现 (图 1:B); 距根尖 30 mm 处, 外皮层细胞较大且形成木栓层, 内皮层凯氏带出现, 邻近内皮层的皮层细胞和皮下厚壁细胞层开始木质化和栓质化 (图 1:C, D); 距根尖 50 mm 处, 内皮层的凯

氏带仍然微弱 (图 1:E), 皮下厚壁组织层和外皮层的细胞壁均木质化、栓质化加厚; 距根尖 70 mm 处, 内皮层的凯氏带发育完全且形成栓质层 (图 1:D, F, H), 随后产生木质化的次生壁 (图 1:H)。

距根尖 5 mm, 菰不定根的皮肤具裂溶生性通气组织 (图 1:A), 距根尖 50 mm, 则形成了细胞以放射状为特点的溶生性通气组织 (图 1:F, G)。在中柱鞘内分别具有 8~12 个原生木质部导管 (图 1:F, G), 2~3 个后生木质部导管 (图 1:A, D, F, G, H)。在老根中, 几乎所有维管柱内细胞都已经木质化为厚壁组织 (图 1:G)。

2.2 地上茎、匍匐茎和根状茎的结构和组织化学

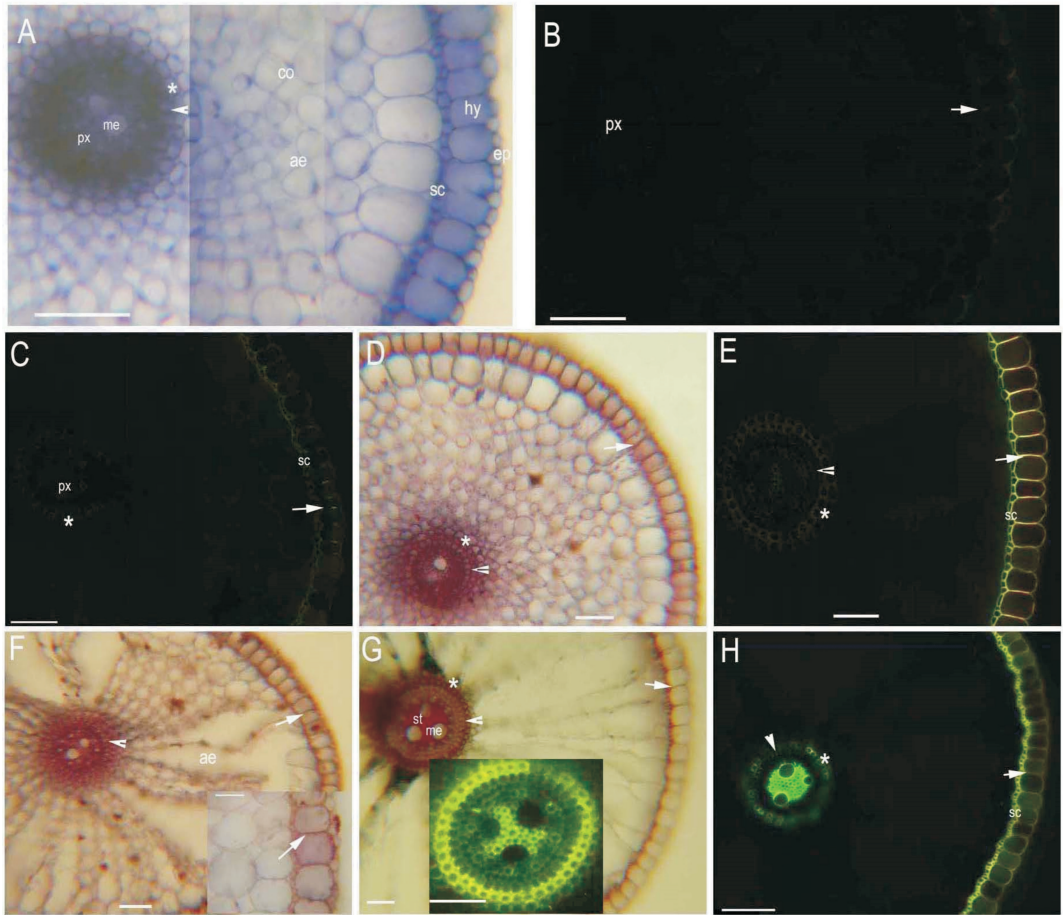
根状茎、匍匐茎和地上茎均有由木质化厚壁细胞组成的周缘厚壁机械组织层 (PMR) 和位于内侧的厚壁组织层 (SCR), 后者常有维管束包埋其中, 并将皮层和维管柱两部分隔开 (图 2:A-H)。周缘厚壁机械组织层 (PMR) 外侧一层细胞有木栓质 (图 2:B, C, E, G) 而无凯氏带 (图 2:A, B)。地上茎、匍匐茎与不定根的解剖结构和通气组织结构都是相似的。幼茎的表皮角质层较厚 (图 2:A); 皮层、中柱、维管束、厚壁组织层和周缘厚壁机械组织层中的许多细胞都呈现栓质化 (Schreiber & Franke, 2011) (图 2:C)。老的地上茎 (图 2:C) 与匍匐茎 (图 2:E) 中的厚壁组织层、维管束、周缘厚壁机械组织层 (图 2:D, F) 以及增厚的角质层 (图 2:B, C) 都含有木栓质。老根状茎的维管束和周缘机械组织层细胞栓质化 (图 2:G), 且木质化 (图 2:H)。

地上茎 (图 2:B, C) 和匍匐茎的气腔 (图 2:E, F) 包括髓腔、皮层和厚壁组织层以内的裂溶生性通气组织。根状茎的气腔包括髓腔和皮层中的裂溶生性通气组织 (图 2:G, H)。

叶鞘和叶片近轴面和远轴面有增厚的角质层 (图 2:I, J), 叶鞘和叶片均有维管束, 由厚壁组织构成的维管束鞘和裂溶生性通气组织 (图 2:I, J)。但叶中的厚壁组织层细胞没有栓质化。

2.3 不定根及根状茎的质外体屏障的通透性检测

通过黄连素示踪法检测不定根和根茎质外体屏障的通透性。在紫外光下, 由外而内, 不定根的表皮、皮下层、内皮层及与之相邻皮层、中柱、根状茎的周缘厚壁机械组织层有较弱自发棕色荧光

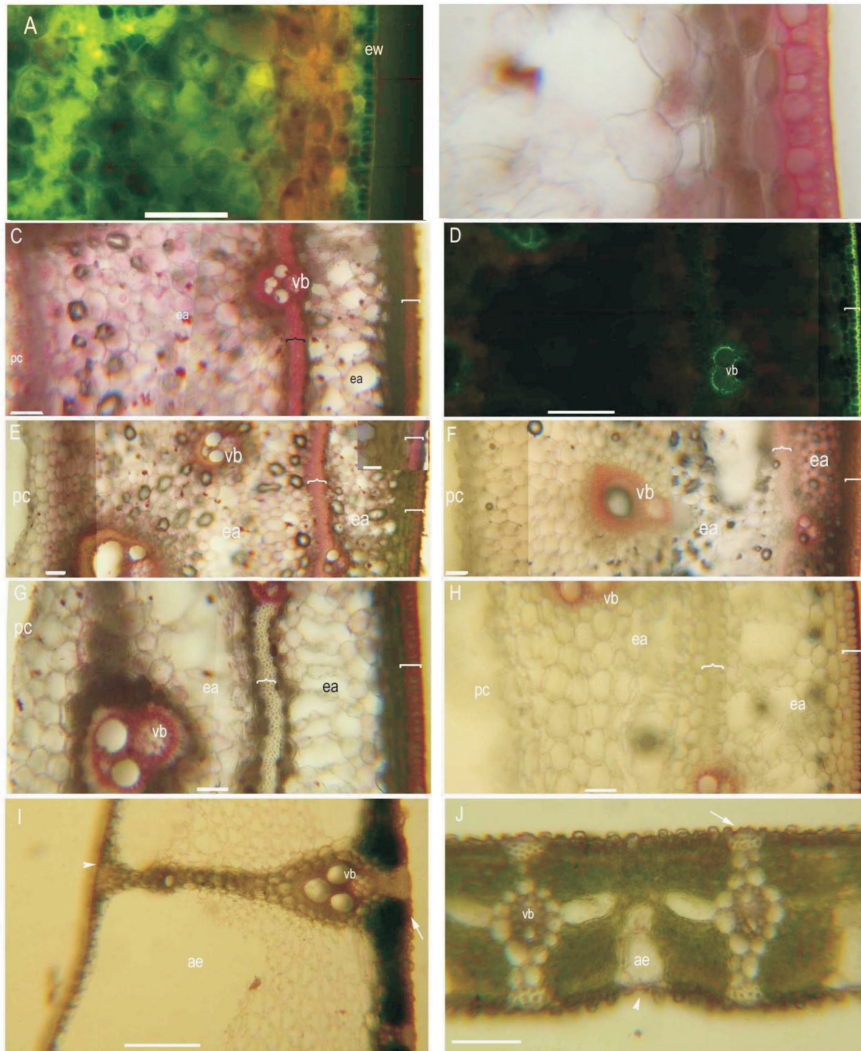


注: **A.** 根长 155 mm, 距根尖 5 mm; 内皮层(箭头); 相邻的具厚壁的皮肤组织(星号); 皮层; 裂溶性通气组织; 皮下组织; 表皮; 厚壁组织层; 原生木质部; 后生木质部; 染色(TBO)。 **B.** 根长 155 mm, 距根尖 10 mm; 带有微弱凯氏带的单层细胞构成的外皮层(箭头); 原生木质部; 染色(BAB)。 **C.** 根长 155 mm, 距根尖 30 mm; 与内皮层相邻的木质化皮层组织(星号); 单层细胞构成的外皮层与凯氏带(箭头); 单层细胞构成的厚壁组织层; 原生木质部; 染色(BAB)。 **D.** 根长 155 mm, 距根尖 30 mm; 内皮层栓质化(箭头); 相邻层内皮层栓质化(星号); 裂溶性通气组织; 栓质化厚壁组织层和外皮层(箭头); 染色(SR7B)。 **E.** 根长 155 mm, 距根尖 50 mm; 内皮层凯氏带(箭头所示); 木质化相邻内皮层(星号); 单层细胞构成的外皮层凯氏带(箭头); 木质化单列厚壁组织层; 染色(BAB)。 **F.** 根长 155 mm, 距根尖 50 mm; 内皮层栓质化(箭头); 裂溶性通气组织; 栓质化厚壁组织层和外皮层(箭头); 染色(SR7B)。 **G.** 根长 155 mm, 距根尖 50 mm; 木质化的内皮层(箭头); 木质化相邻内皮层(星号); 木质化的厚壁组织层和外皮层(箭头); 裂溶性通气组织; 木质化中柱髓细胞; 后生木质部; 染色(盐酸-间苯三酚); 内插图显示原生木质部导管; 染色(黄连素)。 **H.** 根长 155 mm, 距根尖 70 mm; 内皮层凯氏带(箭头所示); 木质化相邻内皮层(星号); 单列外皮层凯氏带(箭头); 木质化单列厚壁组织层; 木质化中柱髓细胞; 染色(BAB)。 **co.** 皮层; **ep.** 表皮; **hy.** 下皮层; **me.** 后生木质部; **px.** 原生木质部; **ae.** 裂溶生的通气组织; **sc.** 厚壁细胞层; **st.** 中柱。 标尺 = 50 μm 。

Note: **A.** Root 155 mm long, sectioned at 5 mm behind tip; endodermis (arrowheads); adjacent endodermal cortical layers with thickened walls (asterisk); cortex; schizolysigeny aerenchyma; hypodermis; epidermis; sclerenchyma layer; protoxylem; metaxylem; staining (TBO). **B.** Root 155 mm long, sectioned at 10 mm; uniseriate exodermis with weakly Casparian bands (arrows); protoxylem; staining (BAB). **C.** Root 155 mm long at 30 mm; lignified adjacent endodermal cortical layers (asterisk); uniseriate exodermis with Casparian bands (arrows); uniseriate SC; staining (BAB). **D.** Root 155 mm long at 30 mm; endodermis suberin lamellae (arrowheads); adjacent endodermal cortical layers suberin lamellae (asterisk); schizolysigeny aerenchyma; suberized SC and exodermis (arrows); staining (SR7B). **E.** Root 155 mm long at 50 mm; endodermis Casparian bands (arrowheads); lignified adjacent endodermal cortical layers (asterisk); uniseriate exodermis Casparian bands (arrows); lignified uniseriate SC; staining (BAB). **F.** Root 155 mm long at 50 mm; endodermis suberin lamellae (arrowheads); schizolysigeny aerenchyma; suberized SC and exodermis (arrows); staining (SR7B). **G.** Root 155 mm long at 50 mm; lignified endodermis (arrowheads); lignified adjacent endodermal cortical layers (asterisk); lignified SC and exodermis (arrows); schizolysigeny aerenchyma; lignified stele pith cells; metaxylem; staining (Pg); inset show protoxylem elements; staining (berberine). **H.** Root 155 mm long at 70 mm; endodermis Casparian bands (arrowheads); lignified adjacent endodermal cortical layers (asterisk); uniseriate exodermis Casparian bands (arrows); lignified uniseriate SC; lignified stele pith cells; staining (BAB). **co.** Cortex; **ep.** Epidermis; **hy.** Hypodermis; **me.** Metaxylem; **px.** Protoxylem; **ae.** Schizolysigenous aerenchyma; **sc.** Sclerenchyma layer; **st.** Stele. Scale bars = 50 μm .

图 1 菰不定根横切片的显微照片

Fig. 1 Photomicrographs of *Zizania latifolia* adventitious roots

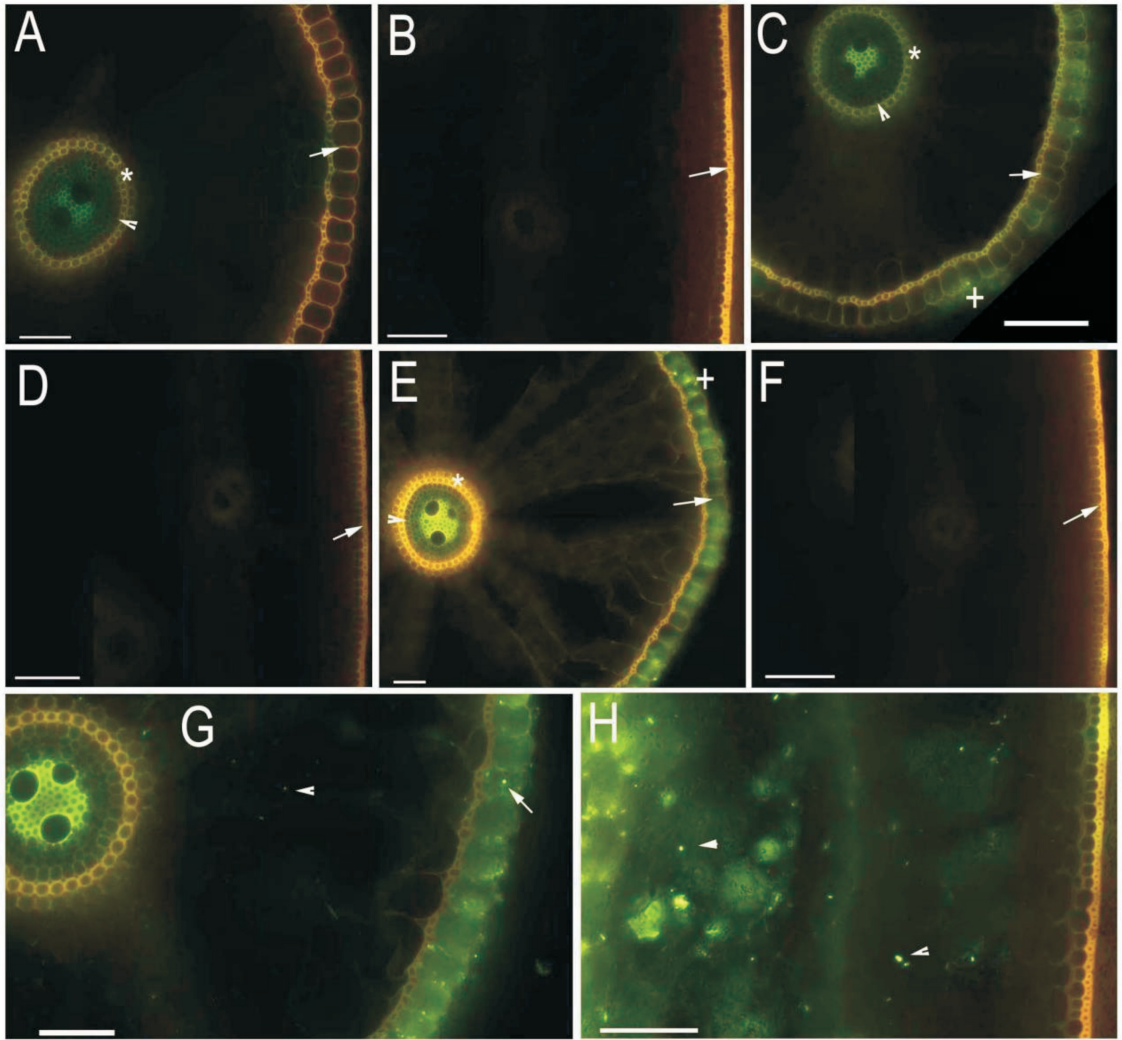


注：A-D. 菰地上茎(长度 200~280 mm, 5~8 节)横切片的显微照片, 分别在第一节间(幼茎)和第三节间(老茎)切片; E, F. 匍匐茎(长度 900 mm, 8-11 节为老茎)切片, 在第一节间切片; G, H. 根状茎(长度 800~910 mm, 20~24 节)切片, 在第五节间切片; I-J. 叶鞘和叶切片; 标尺 = 100 μm 。A. 幼茎, 表皮外切向壁; 染色(BAB)。B. 幼地上茎; 木栓化周缘机械组织层外层与栓质化表皮细胞(); 裂溶生性通气组织; 染色(SR7B); 标尺 = 50 μm 。C. 老地上茎; 栓质化厚壁组织层(); 栓质化周缘机械组织层(); 栓质化维管束细胞; 髓腔; 裂溶生性通气组织; 染色(SR7B)。D. 老地上茎, 木质化的维管束细胞; 木质化周缘机械组织层(); 染色(BAB)。E. 老匍匐茎; 厚壁组织层(); 栓质化维管束; 髓腔; 裂溶生性通气组织; 染色(SR7B); 插图显示, 木栓化周缘机械组织层(); 标尺 = 50 μm 。F. 老匍匐茎; 厚壁组织层(); 木质化维管束细胞; 木质化周缘机械组织层(); 髓腔; 裂溶生性通气组织; 染色(盐酸-间苯三酚)。G. 老根状茎; 厚壁细胞层(); 木栓化周缘机械组织层(); 栓质化维管束细胞; 髓腔; 裂溶生性通气组织; 染色(SR7B)。H. 老根状茎; 厚壁组织层(); 木质化维管束细胞; 木质化周缘机械组织层(); 髓腔; 裂溶生性通气组织; 染色(盐酸-间苯三酚)。I. 叶鞘; 叶鞘近轴面(箭头)和远轴面(箭)的角质层, 木栓化维管束细胞; 裂溶生性通气组织; 染色(SR7B)。J. 叶片; 叶片近轴面(箭头)和远轴面(箭)的角质层; 维管束; 通气组织; 染色(SR7B)。ew. 表皮细胞壁; ae. 裂溶生性通气组织; pc. 髓腔; vb. 维管束。

Note: A-D. Photomicrographs of *Zizania latifolia* culm (200-280 mm long, 5-8 nodes) sectioned at the first internode (young) and at 3th internode (aged); E, F. Stolons (900 mm long, 8-11 nodes are aged) sectioned at the first internode; G, H. Rhizomes (800-910 mm long, 20-24 nodes) sectioned at the 5th internode (aged); I-J. Leaf sheath and leaf sectioned; scale bars = 100 μm . A. Young culm, epidermis outer tangential walls; staining (BAB). B. Young culm, outer layer of PMR with suberin lamellae and suberized epidermis (bracket); schizolysigenous aerenchyma; staining (SR7B); bar = 50 μm . C. Aged culm; suberized SCR (brace); suberized PMR (bracket); suberized vascular bundle cells; pith cavity; schizolysigenous aerenchyma; staining (SR7B). D. Aged culm, lignified vascular bundle cells; lignified PMR (bracket); staining (BAB). E. Aged stolon; SCR (brace); suberized PMR (bracket); suberized vascular bundles; pith cavity; schizolysigenous aerenchyma; staining (SR7B); inset shows suberized PMR (bracket) with suberin lamellae; bar = 50 μm . F. Aged stolon; SCR (brace); lignified vascular bundle cells; lignified PMR (bracket); pith cavity; schizolysigenous aerenchyma; staining (Pg). G. Aged rhizome; SCR (brace); suberized PMR (bracket); suberized vascular bundle cells; pith cavity; schizolysigenous aerenchyma; staining (SR7B). H. Aged rhizome; SCR (brace); lignified vascular bundle cells; lignified PMR (bracket); pith cavity; schizolysigenous aerenchyma; staining (Pg). I. Leaf sheath; cuticle on adaxial surface (arrowhead) and abaxial surface (arrow) of leaf sheath, suberin lamellae on vascular bundle cells; schizolysigenous aerenchyma; staining (SR7B). J. Leaf blade; cuticle on adaxial surface (arrowhead) and abaxial surface (arrow) of leaf blade; vascular bundle; aerenchyma; staining (SR7B). ew. Epidermal cell wall; ae. Schizolysigenous aerenchyma; pc. Pith cavity; vb. Vascular bundle.

图 2 菰茎和叶横切片的显微照片

Fig. 2 Photomicrographs of *Zizania latifolia* adventitious stem and leaf



注: 在长 130 mm 的不定根中截取距顶端 30 mm 到 60 mm 的片段, 两段密封。老的根状茎(地上茎秆和匍匐茎有与之类似的结构和组织化学特征)选取一节间(保留两段的节); 除特别注明外, 标尺 = 100 μm 。A. 不定根通气组织; 相邻的内皮层增厚的皮层(星号), 内皮层(箭头)和外皮层细胞壁(箭头)较弱的棕色; 不染色; 标尺 = 50 μm 。B. 根状茎表皮和周缘机械组织层显示出较弱的棕色(箭头); 不染色。C. 不定根通气组织; 相邻的内皮层增厚的皮层(星号), 内皮层(箭头), 外皮层细胞壁(箭头)黄色荧光; 小檗碱硫氰酸盐晶体(加号)附着在外皮层内外; 小檗碱染色; 标尺 = 50 μm 。D. 根状茎表皮和周缘机械组织层发黄色荧光(箭头); 小檗碱染色。E. 不定根根系通气组织; 增厚的皮层相邻的内皮层(星号), 内皮层(箭头), 外皮层细胞壁(箭头)发黄色荧光; 外皮层内侧和外侧的小檗碱硫氰酸盐晶体(加号); 小檗碱和硫氰酸钾染色。F. 根状茎的表皮细胞和周缘机械组织层发黄色荧光(箭头); 小檗碱和硫氰酸钾染色。G. 不定根破裂的外皮层; 小檗碱硫氰酸盐晶体附着在通气组织(箭头)和外皮层(箭头); 小檗碱和硫氰酸钾染色; 标尺 = 50 μm 。H. 根状茎节间的横截面; 小檗碱盐晶体(箭头)附着通气组织和髓腔中; 小檗碱和硫氰酸钾染色。

Note: Roots segments sectioned at 30 mm to 60 mm from the tip of 130 mm long roots and sealed ends. The aged rhizome (as stem representative for culms and stolons have similar structure and histochemistry) samples excised with one internode and two end nodes and not sealed ends; except where noted, scale bars = 100 μm . A. Roots with aerenchyma; thickened adjacent endodermal cortical layers (asterisk), endodermis (arrowhead) and exodermis (arrow) cell walls faintly brown; unstained; bar = 50 μm . B. Epidermis and PMR of rhizomes faintly brown (arrow); unstained. C. Roots with aerenchyma; thickened adjacent endodermal cortical layers (asterisk), endodermis (arrowhead) and exodermis cell walls (arrow) fluoresced yellow; crystals of berberine thiocyanate (cross) enter into exodermis or out of it; berberine stained; bar = 50 μm . D. Epidermis and PMR of rhizomes fluoresced yellow (arrow); berberine stained. E. Roots with aerenchyma; thickened adjacent endodermal cortical layers (asterisk), endodermis (arrowhead), and exodermis cell walls (arrow) fluoresced yellow; crystals of berberine thiocyanate (cross) enter into exodermis or out of it; berberine and KSCN stained. F. Epidermis and PMR of rhizomes fluoresced yellow (arrow); berberine and KSCN stained. G. Roots with ruptured exodermis; crystals of berberine thiocyanate enter into aerenchyma (arrowhead) and exodermis (arrow); berberine and KSCN stained; bar = 50 μm . H. Transverse sections of rhizomes internodes; crystals of berberine thiocyanate (arrowhead) adhere to aerenchyma and pith cavity; berberine and KSCN stained.

图 3 菰不定根和根状茎的质外体屏障通透性试验

Fig. 3 Apoplastic barriers permeability tests on roots and rhizomes of *Zizania latifolia*

(图 3:A,B)。仅黄连素处理切段,不定根的内皮层细胞壁和皮下层、茎的表皮和周缘厚壁机械组织层有较弱自发棕色荧光,硫氰酸黄连素晶体附着在不定根外皮层细胞壁上,不定根的皮下厚壁组织层自发强烈黄色荧光(图 3:C,D)。

黄连素和硫氰酸钾处理切段,不定根的内皮层和厚壁组织层的细胞壁、根状茎的表皮强烈吸收黄连素而具强烈橙色荧光(图 3:E,F);观察没有用硫氰酸黄连素晶体染色的通气组织,发现不定根破裂的外皮层内部存在一些晶体(图 3:E);黄连素和硫氰酸钾处理后,不定根和根状茎节间外皮层破裂,内部具硫氰酸黄连素晶体而自发强烈黄色荧光(图 3:G,H),不定根中央厚壁组织自发强烈黄色荧光(图 3:E,G)。该研究表明不定根外皮层及厚壁组织层能吸收阻挡离子进入皮层及内部,根状茎表皮及外皮层吸收阻挡离子进入。

3 讨论

近年来,我们主要研究了江汉平原既能耐水湿又能早生的植物的解剖结构和组织化学特征,如狗牙根(*Cynodon dactylon*)、双穗雀稗(*Paspalum paspaloides*)、假俭草(*Eremochloa ophiuroides*)、牛鞭草(*Hemarthria altissima*)、白茅(*Imperata cylindrica*) (杨朝东等,2015;杨朝东和张霞,2013;张霞等,2013)。国外主要报道了水稻(*Oryza sativa*)、水甜茅(*Glyceria maxima*)、梭鱼草(*Pontederia cordata*)、芦苇(*Phragmites australis*)、荻(*Triarrhena sacchariflora*)和香蒲(*Typha orientalis*)的不定根和根茎的解剖结构和组织化学(Soukup et al., 2007; Seago et al., 1999; Mcmanus et al., 2002; Watanabe et al., 2006)。

本研究中,菰不定根解剖结构由外而内依次为表皮、外皮层、厚壁机械组织层、皮层、内皮层和维管柱。其屏障结构由位于内侧的内皮层及其邻近栓质化细胞和外侧的外皮层组成。这与已报道湿地植物狗牙根、双穗雀稗、白茅、水稻、芦苇等的研究结果相同(Yang et al., 2011; 张霞等,2013; Watanabe et al., 2006; Simone et al., 2003)。关于植物物质外体屏障结构,菰的内皮层在草本植物根

中最具典型特征(Yang et al., 2011)。其根的外皮层与水甜茅类似(Soukup et al., 2007),但水甜茅的外皮层有增厚的次生细胞壁,而没有厚壁机械组织层。菰根的通气组织大多为放射状溶原性,许多其他湿地物种也有此典型特征(Seago et al., 2005; Jung et al., 2008; Sangster, 1985)。这说明菰和其他适应湿地和干旱层境的植物具相似屏障结构。

菰茎(包括匍匐茎、根状茎和地上茎)的解剖结构由外向内依次为角质层、表皮、周缘厚壁机械组织层、皮层、厚壁组织层和髓腔。通气组织包括皮层通气组织和髓腔。茎具内侧厚壁机械组织层,外侧的角质层和周缘厚壁机械组织层组成的屏障结构,屏障结构的细胞壁具凯氏带、木栓质和木质素沉积的组织化学特点。菰茎与狗牙根、双穗雀稗、牛鞭草、假俭草的茎有些不同:一方面,菰茎有木质化和栓质化的周缘厚壁机械组织层。草本植物的茎和叶多有木栓质晶体的存在(Fahn, 1990; Evert et al., 1996)。菰茎的维管束细胞木质化且栓质化,而在狗牙根、假俭草、双穗雀稗和牛鞭草中其维管束细胞则仅木质化,但菰茎木质化的周缘厚壁机械组织层和厚壁组织层比狗牙根和双穗雀稗等的细胞层数少,说明菰属于湿生,可以短暂缺水,但不能早生。原因在于厚壁组织层较薄,失水过多和时间长,细胞缺水而易死亡。另一方面,菰地上茎(秆)和匍匐茎有木质化和明显栓质化的厚壁组织层,而狗牙根、假俭草、双穗雀稗和牛鞭草的厚壁组织层仅木质化(Yang et al., 2011)。与其他禾本科植物(如水甜茅等)不同(Metcalf, 1960),菰茎中具连接维管束内层的厚壁细胞层;香蒲没有具有凯氏带的外皮层和内皮层(Yang et al., 2011);菰匍匐茎的表皮细胞与香蒲、狗牙根等具匍匐茎的禾草相似(Yang et al., 2011; Mcmanus et al., 2002),有增厚的角质层,不同点在于,其表皮细胞很少栓质化(Schreiber & Franke, 2011)。

菰的通气组织包括根中通气组织,茎皮层通气组织和髓腔,与狗牙根、假俭草、牛鞭草、荻类似(Seago et al., 2005; Jung et al., 2008; Yang et al., 2011; Sangster, 1985)。菰茎和叶皮层中的裂溶

生通气组织的溶解是很正常的现象,显然,这些不断形成的气腔(Kawai et al., 1998),有助于植物在缺氧环境中把氧气储存和运输到其他器官(Armstrong et al., 2006; Vartapetian & Jackson, 1997),是其有效地适应湿地环境的特征。

菰茎的质外体屏障主要存在于根外皮层和内皮层,以及茎的周缘厚壁机械组织层。这些屏障使菰与狗牙根、假俭草、牛鞭草、芦苇、双穗雀稗和香蒲这些典型的湿地植物具有很多相似之处,但是茎周缘厚壁机械组织层与狗牙根等植物相比层数少,内部厚壁机械组织层也没有狗牙根等发达,推测菰在旱生环境条件下,周缘厚壁机械组织层和厚壁机械组织层保护组织对植物体的保护很有限,容易失水,不能保持植物体固有姿态(Meyer et al., 2009; Mcmanus et al., 2002; 谭淑端等, 2009; Yang et al., 2011; 王海锋等, 2008)。在湿地环境下,菰这些屏障保护结构可以有效阻碍植物体与环境之间的氧和离子的自由扩散(Meyer et al., 2011; Krishnamurthy et al., 2011)。

总之,通过对菰的解剖结构和组织化学特征的研究,比较其他湿地植物和两栖植物适应水生和旱生生境的解剖结构特征,菰茎的周缘厚壁机械组织层和厚壁组织层较薄,在旱生环境下易失水,不能保持内部细胞固有姿态而不能抵御干旱环境,明确其在湿地环境中分布有一定的局限性。通过对菰营养体解剖结构的研究,对有效利用这些湿地植物资源,恢复三峡库区消落带、江汉平原退化湿地植被具有重要参考价值。

参考文献:

ARMSTRONG W, COUSINS D, ARMSTRONG J, et al., 2000. Oxygen distribution in wetland plant roots and permeability barriers to gas-exchange with the rhizosphere: A micro-electrode and modelling study with *Phragmites australis* [J]. *Ann Bot*, 86(3): 687-703.

ARMSTRONG J, JONES RE, ARMSTRONG W, 2006. Rhizome phyllosphere oxygenation in *Phragmites* and other species in relation to redox potential, convective gas flow, submergence and aeration pathways [J]. *New Phytol*, 172(4): 719-731.

BRUNDRETT MC, ENSTONE DE, PETERSON CA, 1988. A

berberine-aniline blue fluorescent staining procedure for suberin, lignin, and callose in plant tissue [J]. *Protoplasma*, 146(2-3): 133-142.

BRUNDRETT MC, KENDRICK B, PETERSON CA, 1991. Efficient lipid staining in plant material with Sudan Red 7B or fluoral yellow 088 in polyethylene glycol-glycerol [J]. *Bio-technol Histochem*, 66(3): 111-116.

COLMER TD, 2003. Aerenchyma and an inducible barrier to radial oxygen loss facilitate root aeration in upland, paddy and deep-water rice (*Oryza sativa* L.) [J]. *Ann Bot*, 91(2): 301-309.

ENSTONE DE, PETERSON CA, MA F, 2002. Root endodermis and exodermis structure, function, and responses to the environment [J]. *J Plant Growth Regul*, 21(4): 335-351.

EVERT RF, RUSSIN WA, BOSABALIDIS AM, 1996. Anatomical and ultrastructural changes associated with sink-to-source transition in developing maize leaves [J]. *Int J Plant Sci*, 157(3): 247-261.

FAHN A, 1990. *Plant Anatomy* [M]. Oxford, UK: Pergamon Press: 1-544.

JENSEN WA, 1962. *Botanical histochemistry-principles and practice* [M]. W. H. Freeman, San Francisco, Calif, USA: 1-408.

JORGENSEN KD, LEE PE, KANAVILLIL K, 2013. Ecological relationships of wild rice, *Zizania* spp. 11. Electron microscopy study of iron plaques on the roots of northern wild rice (*Zizania palustris*) [J]. *Bot*, 91(3): 189-201.

JUDZIEWICZ EJ, CLARK LG, 2007. Classification and biogeography of New World Grasses: Anomochloioideae, Pharioideae, Ehrhartoideae, and Bambusoideae [J] // COLUMBUS JT, FRIAR EA, PORTER JM, et al. *Monocots: Comparative Biology and Evolution* Poales. Claremont CA. USA: Rancho Santa Ana Bot Gard, 23(1): 303-314.

JUNG J, LEE SC, CHO HK, 2008. Anatomical patterns of aerenchyma in aquatic and wetland plants [J]. *J Plant Biol*, 51(6): 428-439.

KAWAI M, SAMARAJEEVA PK, BARRERO RA, 1998. Cellular dissection of the degradation pattern of cortical cell death during aerenchyma formation of rice roots [J]. *Planta*, 204(3): 277-287.

KOTULA L, RANTHUNGRE K, SCHREIBER L, et al., 2009. Functional and chemical comparison of apoplastic barriers to radial oxygen loss in roots of rice (*Oryza sativa* L.) grown in aerated or deoxygenated solution [J]. *J Exp Bot*, 60(7): 2155-2167.

KRISHNAMURTHY P, RANATHUNGE K, NAYAK S, et al., 2011. Root apoplastic barriers block Na⁺ transport to shoots in rice (*Oryza sativa* L.) [J]. *J Exp Bot*, 62(12): 4215-4228.

MCMANUS HA, SEAGO JR JL, MARSH LC, 2002. Epifluorescent and histochemical aspects of shoot anatomy of *Typha latifolia* L., *Typha angustifolia* L. and *Typha glauca* Godr. [J]. *Ann Bot*, 90(4): 489-493.

- METCALFE CR, 1960. Anatomy of the Monocotyledons. I. Gramineae [M]. London, UK: Oxford University Press; 1-731.
- MEYER CJ, PETERSON CA, 2011. Casparian bands occur in the periderm of *Pelargonium hortorum* stem and root [J]. *Ann Bot*, 107(4): 591-598.
- MEYER CJ, SEAGO JR JL, PETERSON CA, 2009. Environmental effects on the maturation of the endodermis and multi-seriate exodermis of *Iris germanica* roots [J]. *Ann Bot*, 103(5): 687-702.
- RANTHUNGRE K, LIN J, STEUDLE E, et al., 2011. Stagnant deoxygenated growth enhances root suberization and lignifications, but differentially affects water and NaCl permeabilities in rice (*Oryza sativa* L.) roots [J]. *Plant Cell Environ*, 34(8): 1223-1240.
- SANGSTER AG, 1985. Silicon distribution and anatomy of the grass rhizome, with special reference to *Miscanthus sacchariflorus* (Maxim.) Hackel [J]. *Ann Bot*, 55(5): 621-634.
- SCHREIBER L, FRANKE RB, 2011. Endodermis and exodermis in roots [J]. Chichester, UK: John Wiley & Sons, Ltd. <http://www.els.net> [doi: 10.1002/9780470015902.a0002086.pub2.]
- SCULTHORPE CD, 1967. The biology of aquatic vascular plants [M]. London, UK: Edward Arnold Ltd; 1-610.
- SEAGO JR JL, MARSH LC, STEVENS KJ, et al., 2005. A re-examination of the root cortex in wetland flowering plants with respect to aerenchyma [J]. *Ann Bot*, 96(4): 565-579.
- SEAGO JR JL, PETERSON CA, ENSTONE DE, et al., 1999. Development of the endodermis and hypodermis of *Typha glauca* Godr. and *T. angustifolia* L. roots [J]. *Can J Bot*, 77(1): 122-134.
- SEAGO JR JL, PETERSON CA, ENSTONE DE, 2000. Cortical development in roots of the aquatic plant *Pontederia cordata* (Pontederiaceae) [J]. *Am J Bot*, 87(8): 1116-1127.
- SIMONE OD, HAASE K, MÜLLER E, et al., 2003. Apoplastic barriers and oxygen transport properties of hypodermal cell walls in roots from four Amazonian tree species [J]. *Plant Physiol*, 132(1): 206-217.
- SOUKUP A, ARMSTRONG W, SCHREIBER L, et al., 2007. Apoplastic barriers to radial oxygen loss and solute penetration: A chemical and functional comparison of the exodermis of two wetland species, *Phragmites australis* and *Glyceria maxima* [J]. *New Phytol*, 173(2): 264-278.
- STOVER EL, 1928. The roots of wild rice *Zizania aquatica* L. [J]. *Ohio J Sci*, 28(1): 43-49.
- STOVER EL, 1951. An introduction to the anatomy of seed plants [J]. *Aibs Bull*, 1(2): 10.
- TAN SD, ZHU MY, DANG HS, et al., 2009. Physiological responses of bermudagrass (*Cynodon dactylon* L. Pers.) to deep submergence stress in the Three Gorges Reservoir Area [J]. *Acta Ecol Sin*, 29(7): 3685-3692. [谭淑端, 朱明勇, 党海山, 等, 2009. 三峡库区狗牙根对深淹胁迫的生理响应 [J]. *生态学报*, 29(7): 3685-3692.]
- TATEOKA T, 1969. Root anatomy in grass systematic [J]. *Bull Nat Sci Museum*, 12(3): 643-651.
- VARTAPETIAN BB, JACKSON MB, 1997. Plant adaptations to anaerobic stress [J]. *Ann Bot*, 79(Suppl. 1): 3-20.
- WANG HF, ZENG B, LI Y, et al., 2008. Effects of long-term submergence on survival and recovery growth of four riparian plant species in Three Gorges Reservoir region [J]. *Chin J Plant Ecol*, 32(5): 977-984. [王海锋, 曾波, 李娅, 等, 2008. 长期完全水淹对 4 种三峡库区岸生植物存活及恢复生长的影响 [J]. *植物生态学报*, 32(5): 977-984.]
- WATANABE H, SAIGUSA M, MORITA S, 2006. Identification of casparian bands in the mesocotyl and lower internodes of rice (*Oryza sativa* L.) seedlings using fluorescence microscopy [J]. *Plant Prod Sci*, 9(4): 390-394.
- YANG CD, LI SF, DENG SM, et al., 2015. Study of the anatomy and apoplastic barrier characteristics of *Imperata cylindrica* [J]. *Acta Pratac Sin*, 24(3): 213-218. [杨朝东, 李守峰, 邓仕明, 2015. 白茅解剖结构和屏障结构特征研究 [J]. *草业学报*, 24(3): 213-218.]
- YANG CD, ZHANG X, 2013. The permeability and supplement structures in stems for *Paspalum distichum* [J]. *Bull Bot Res*, 33(5): 564-568. [杨朝东, 张霞, 2013. 双穗雀稗 (*Paspalum distichum*) 通透性生理和茎解剖结构补充研究 [J]. *植物研究*, 33(5): 564-568.]
- YANG CD, ZHANG X, LIU GF, et al., 2013. Progress on the structure and physiological function of apoplastic barriers in root [J]. *Bull Bot Res*, 33(1): 114-119. [杨朝东, 张霞, 刘国锋, 等, 2013. 植物根中质外体屏障结构和生理功能研究进展 [J]. *植物研究*, 33(1): 114-119.]
- YANG CD, ZHANG X, ZHOU CY, 2011. Root and stem anatomy and histochemistry of four grasses from the Jiangnan Floodplain along the Yangtze River, China [J]. *Flora*, 206(7): 653-661.
- ZHANG X, YANG CD, NING GG, 2013. The comparison development of apoplastic barriers in *Cynodon dactylon* and *Paspalum distichum* roots [J]. *Hubei Agric Sci*, 52(20): 4991-4994. [张霞, 杨朝东, 宁国贵, 2013. 狗牙根和双穗雀稗根中质外体屏障结构发育过程的比较研究 [J]. *湖北农业科学*, 52(20): 4991-4994.]